I S A V

Journal of Theoretical and Applied Vibration and Acoustics

journal homepage: http://tava.isav.ir

Nonlinear dynamic analysis of a four-bar mechanism having revolute joint with clearance

Sajjad Boorghan Farahan, MohammadReza Ghazavi*, Sasan Rahmanian

Department of Mechanical Engineering, Tarbiat Modares University, Jalal Al Ahmad, Nasr Bridge, Postal Code: 14115-143, Tehran, Iran.

ARTICLE INFO

Article history:
Received 4 February 2016

Received in revised form
18 April 2016

Accepted 23 April 2016

Available online 25 May 2016

Keywords:
Four-bar linkage

Clearance

Poincaré portrait

Bifurcation

Chaos

ABSTRACT

In general, joints are assumed without clearance in the dynamic analysis of multi-body mechanical systems. When joint clearance is considered, the mechanism obtains two uncontrollable degrees of freedom and hence the dynamic response considerably changes. The joints' clearances are the main sources of vibrations and noise due to the impact of the coupling parts in the joints. Therefore, the system responses lead to chaotic and unpredictable behaviors instead of being periodic and regular. In this paper, nonlinear dynamic behavior of a four-bar linkage with clearance at the joint between the coupler and the rocker is studied. The system response is performed by using a nonlinear continuous contact force model proposed by Lankarani and Nikravesh [1] and the friction effect is considered by a modified Coulomb friction law [2]. By using the Poincaré portrait, it is proven that either strange attractors or chaos exist in the system response. Numerical simulations display both periodic and chaotic motions in the system behavior. Therefore, bifurcation analysis is carried out with a change in the size of the clearance corresponding to different values of crank rotational velocities. Fast Fourier Transformation is applied to analyze the frequency spectrum of the system response.

1. Introduction

Over the last few decades, the dynamic modelling of multi-body systems has been identified as an important tool in the analysis, design, optimization, control and simulation of complex mechanisms. Clearance may cause severe vibration, noise and affect the dynamic properties and accuracy of the mechanism response. Therefore, it is very important to study the clearance effect on the dynamics of machine systems. Linkage with clearance is a high-order nonlinear time varying system which is difficult to be analysed.

A great number of researches have been conducted to investigate the effect of joint clearance on the dynamic response of mechanical systems [3-15]. Dubowsky [16, 17] developed an impact

* Corresponding Author: Mohammad Reza Ghazavi, Email: ghazavim@modares.ac.ir

pair model to describe the joint clearance in mechanisms. The model divided the contact between the journal and bearing of a joint linkage into two categories named the contact and noncontact phases. Rhee and Akay [18] investigated the dynamic response of a four-bar mechanism with revolute clearance joint. Haines [19] investigated the dynamic response of the revolute joints with clearance experimentally. Using the massless model, the study by Senviratne and Earles [20] showed that chaotic behavior is exhibited in the dynamic response of a linkage with clearance. Schwab et al. [21] compared different revolute joint clearance models in the dynamic analysis of rigid and elastic mechanical systems. The hydrodynamic lubrication model, in this case, was based on the Reynolds equation for a thin film, incorporating the finite length of the bearing and the effect of cavitation in the fluid film. Flores [22-24] analyzed the stabilizing effects of lubrication in a clearance joint on the dynamic behavior of mechanisms. Flores and Lankarani [24] investigated spatial rigid multi-body lubricated systems with spherical clearance joints. They also presented a general methodology for dynamic modeling and analysis of the planar multi-body systems with multiple clearance joints [25]. Muvengei et al. [12] investigated multi-body systems with clearance and without the friction effect to obtain and characterize the slip-stick effects. Daniel and Cavalca [26] studied the dynamics of a slider-crank mechanism with hydrodynamic lubrication in the clearance of connecting rod-slider joint. Tang et al. [9] studied the nonlinear dynamic behavior of a four-bar linkage considering clearance. Koshy et al. [27] investigated the effects of crank rotational velocity and clearance size on the dynamic response of a slider-crank mechanism both numerically and experimentally. They proved that the slider acceleration amplitude increases by increasing the two parameters. Bai et al. [28] simulated the wear phenomenon in a four-bar mechanism with joint clearance by utilizing Archard's wear model. Tian et al. [29] proposed a comprehensive method for dynamic analysis of a geared multi-body system supported by Elasto Hydro Dynamic (EHD) lubricated cylindrical joints. Askari et al. [30] studied the effect of friction-induced vibration and contact mechanics on the maximum contact pressure and moment of artificial hip implants.

In order to eliminate the contact loss between the journal and the bearing, a controlling mechanism based on the DFC method is proposed by Olyaei and Ghazavi [11]. An optimization method is proposed to alleviate the undesirable effects of joint clearance by Varedi et al. [3]. The study has optimized the mass distribution of the links for a slider-crank mechanism in order to reduce or eliminate the impact forces in the journal-bearing system. Bifurcation analyses with the change of clearance size are carried out by Rahmanian and Ghazavi [4].

In this paper, bifurcation and chaos phenomena are investigated in a four-bar mechanism with an imperfect joint. First, the set of motion equations governing the system's dynamics are established. Then, the solutions are obtained through applying the fourth order adaptive Runge-Kutta method. A MATLAB code is developed for numerical simulation of the equations. It is shown that strange attractors exist in the discrete time domain when the system exhibits a chaotic motion. This behavior appears for low values of input crank velocity.

The main purpose of this research is stability analysis of the multi-body mechanical system with revolute clearance joint through bifurcation diagrams. The Poincaré portraits and FFT plots are prepared for some specific values of the mentioned parameters in order to demonstrate the periodic and chaotic behaviors of the mechanism.

2. Kinematic analysis

In this section, normal and tangential relative velocities of the contact points are calculated by considering a continuous contact mode in the journal-bearing system. The schematic diagram of a revolute clearance joint is shown in Fig. 1. Radial clearance is introduced as the difference between the journal and bearing radii as:

$$c = R_B - R_J \tag{1}$$

where R_J and R_B are the journal and bearing radii respectively and c indicates the clearance size. The contact between journal and bearing is recognized when Eq. 2 is satisfied.

$$\delta = r - (\mathrm{R}_B - \mathrm{R}_J) \geq 0 \tag{2}$$

where r is the magnitude of the clearance vector and δ represents the relative penetration depth between the colliding bodies.

$\vec{r}_P^{\,B}$ and $\vec{r}_P^{\,J}$ vectors represent the position of contact points on the bearing and journal in the global reference frame XY given by:

$$\vec{r}_P^{\,B} = \vec{r}_O^{\,B} + \vec{r}_{P/0}^{\,B} \tag{3}$$

$$\vec{r}_P^{\,J} = \vec{r}_O^{\,J} + \vec{r}_{P/0}^{\,J} \tag{4}$$

$$\vec{r}_P^{\,B/J} = \vec{r}_O^{\,B} - \vec{r}_O^{\,J} + \vec{r}_{P/0}^{\,B} - \vec{r}_{P/0}^{\,J} \tag{5}$$

As illustrated in Fig. 1, $\vec{r}_O^{\,B} - \vec{r}_O^{\,J} = -r\vec{n}$. Relative velocity of the contact point can be calculated by differentiating Eq. 5 as follows:

$$\vec{v}_P^{\,B/J} = -\dot{r}\vec{n} + \left(\omega_B R_B - \omega_J R_J - r\dot{\alpha}\right)\vec{t} \tag{6}$$

ω_J and ω_B are the journal and bearing angular velocities respectively and α represents the orientation of the clearance vector $\vec{r}$ from the positive X axis.

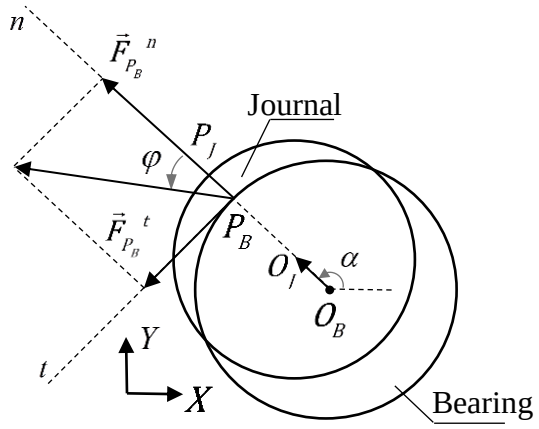

Fig. 1: Normal and tangential contact forces

3. Normal and tangential contact forces

One of the most well-known contact force models which is frequently used in multi-body mechanical systems is proposed by Lankarani and Nikravesh [1]. This is a nonlinear viscoelastic contact force model and is utilized to model the normal contact force between the journal and the bearing.

The normal contact force model is as follows [1]:

$$F_N = K\delta^n \left[1 + \frac{3\left(1 - c_r{}^2\right)}{4} \frac{\dot{\delta}}{\dot{\delta}^{(-)}} \right] \tag{7}$$

where K is the generalized stiffness, δ represents the relative penetration depth between the colliding bodies, c_r is the restitution coefficient and the exponent n is set to 1.5 for the case there is a parabolic distribution of contact stresses in circular and elliptical contacts [11]. $\dot{\delta}$ is the relative normal velocity of contact points and $\dot{\delta}^{(-)}$ indicates the initial impact velocity which remains constant during each contact process.

The generalized stiffness K is a function of the radius and material properties of the spheres i and j and is written as:

$$K = \frac{4}{3(\sigma_i + \sigma_j)} \sqrt{\left(\frac{R_i R_j}{R_i + R_j}\right)} \tag{8}$$

Here σ_i and σ_j are material parameters given by:

$$\sigma_k = \frac{1 - \upsilon_k{}^2}{E_k}, \; K = i, j \tag{9}$$

In Eq. 9, E_k and υ_k are the Young's modulus and the Poisson's ratio of the journal and bearing respectively.

It is worth to mention that in Eq. 8, the curvature radius of the contact profiles is positive for convex surfaces and negative for concave surfaces. Generally, this model is suitable for most mechanical contact problems especially in cases where the energy dissipation during contact process is relatively low in comparison with the maximum elastic energy absorbed. In other words, Eq. 7 is more reliable when the restitution coefficient is close to unity.

Furthermore, the friction force is applied to the system when the tangential component of the relative velocity of the colliding points is not negligible. The modified Coulomb's friction law is expressed by Ambrósio [2]:

$$\vec{f}_t = -c_f c_d F_n \frac{\vec{V}_t}{\left|\vec{V}_t\right|} \tag{10}$$

where c_d is the dynamic correction coefficient,

$$c_d = \begin{cases} 1 & v_t < v_0 \\ \dfrac{v_t - v_0}{v_1 - v_0} & v_0 < v_t \le v_1 \\ 0 & v_t > v_1 \end{cases} \tag{11}$$

in where v_0 and v_1 are the tangential velocity tolerances. The dynamic correction factor c_d prevents the friction force from changing direction for almost null values of tangential velocity. This is contemplated by the integration algorithm as a dynamic response with high frequency contents and thereby, forcing a reduction in the time step size.

According to the models proposed by Lankarani et al. [1] and Ambrósio [2], the resultant contact force on the bearing is:

$$Q_C = K\sqrt{1 + {c_f}^2 {c_d}^2}\left(r - \left(R_B - R_J\right)\right)^{\frac{3}{2}}\left(1 + \frac{3\left(1 - {c_r}^2\right)}{4}\frac{\dot{r}}{\dot{r}^{(-)}}\right) \tag{12}$$

Introducing Q_c as the magnitude of the contact force and ψ as its orientation, then:

$$\varphi = \tan^{-1}\left(-c_f c_d \frac{\omega_B R_B - \omega_J R_J - r\dot{\alpha}}{\left|\omega_B R_B - \omega_J R_J - r\dot{\alpha}\right|}\right),\ \psi = \alpha + \varphi \tag{13}$$

According to the Fig. 2, r and α can be calculated as follows:

$$r=\sqrt{X_{rel}{}^2+Y_{rel}{}^2}=\left[\left(L_1-L_2\cos\theta_2-L_3\cos\theta_3+L_4\cos\theta_4\right)^2+\left(L_4\sin\theta_4-L_2\sin\theta_2-L_3\sin\theta_3\right)^2\right]^{\frac{1}{2}} \tag{14}$$

$$\alpha=\tan^{-1}\left(\frac{Y}{X}\right)=\tan^{-1}\left(\frac{L_4\sin\theta_4-L_2\sin\theta_2-L_3\sin\theta_3}{L_1-L_2\cos\theta_2-L_3\cos\theta_3+L_4\cos\theta_4}\right) \tag{15}$$

Time differentiation on Eqs. 14 and 15 gives $\dot{r}$ and $\dot{\alpha}$ in the matrix form as:

$$\begin{bmatrix}\dot{r}\\ \dot{\alpha}\end{bmatrix}=\begin{pmatrix}\cos\alpha & -r\sin\alpha\\ \sin\alpha & r\cos\alpha\end{pmatrix}^{-1}\begin{bmatrix}L_2\omega\sin\theta_2+L_3\dot{\theta}_3\sin\theta_3-L_4\dot{\theta}_4\sin\theta_4\\ L_4\dot{\theta}_4\cos\theta_4-L_2\omega\cos\theta_2-L_3\dot{\theta}_3\cos\theta_3\end{bmatrix} \tag{16}$$

4. Equations of motion

Figure 2 illustrates a four-bar mechanism with revolute clearance joint in connection of the coupler and the rocker. The clearance magnitude is magnified in order to better comprehend the problem. Each revolute joint with clearance removes two kinematic constrains, hence, this mechanism is a three-degree-of-freedom linkage. Therefore, dynamics of the journal inside the bearing is controlled by the impact-contact forces. Generalized coordinates to set the system configuration is $q=[\theta_2;\theta_3;\theta_4]$.

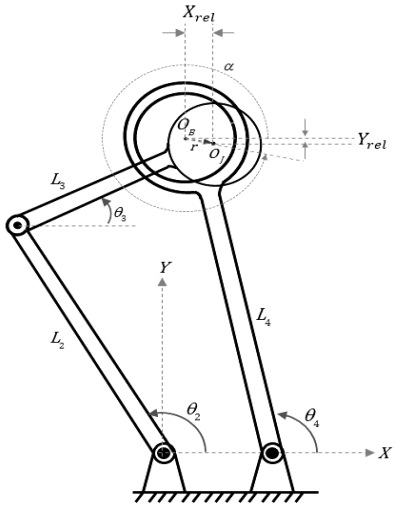

Fig 2: Four-bar mechanism with revolute clearance joint between the coupler and rocker.

The Lagrangian equations for the motion of an unconstrained dynamical system are in the form:

$$\frac{d}{dt}\left(\frac{\partial L}{\partial \dot{q}_k}\right)-\frac{\partial L}{\partial q_k}=Q_{nc,k} \quad ; \quad k=2,3,4 \tag{17}$$

where $L=T-U$ is the Lagrangian function. T and U are the system kinetic and potential energies respectively. $Q_{nc,k}$ is the non-conservative generalized force corresponding to the generalized coordinate q_k and can be calculated as:

$$Q_{nc,k}=\sum_{i=2}^{4}\left(\vec{F}_i^{*}.\frac{\partial \vec{V}_{c,i}}{\partial \dot{q}_k}+\vec{M}_i^{*}.\frac{\partial \vec{\omega}_i}{\partial \dot{q}_k}\right) \tag{18}$$

In Eq. 18, $\vec{F}_i^{*}$ and $\vec{M}_i^{*}$ are the resultants of the external forces and moments acting on the mass center of the body i respectively. $\vec{V}_{c,i}$ and $\vec{\omega}_i$ are the translational and rotational velocities for the mass center of the body i respectively. Using Eq. 18, the generalized forces can be written as follows:

$$\begin{aligned} Q_{\theta_2}&=L_2Q_c\sin(\gamma-\theta_2)+M_2 \\ Q_{\theta_3}&=Q_c\left(L_3\sin(\gamma-\theta_3)+R_i\sin\varphi\right) \\ Q_{\theta_4}&=Q_c\left(L_4\sin(\theta_4-\gamma)-R_j\sin\varphi\right) \end{aligned} \tag{19}$$

In Eq. 19, M_2 is the external moment asserted on the crank.

Kinetic and potential energies of the system are written as follows:

$$T=\frac{1}{2}\left(I_{G2}+\frac{1}{4}m_2L_2^2\right)\omega_2^2+\frac{1}{2}I_{G3}\dot{\theta}_3^2+\frac{1}{2}m_3\left[L_2^2\omega_2^2+\frac{1}{4}L_3^2\dot{\theta}_3^2+L_2L_3\omega_2\dot{\theta}_3\cos(\theta_2-\theta_3)\right]+\frac{1}{2}\left(I_{G4}+\frac{1}{4}m_4L_4^2\right)\dot{\theta}_4^2 \tag{20}$$

$$U=\frac{1}{2}m_2gL_2\sin\theta_2+m_3g\left(L_2\sin\theta_2+\frac{1}{2}L_3\theta_3\right)+\frac{1}{2}m_4gL_4\sin\theta_4 \tag{21}$$

The Lagrangian function is:

$$L = T - U = \frac{1}{2}\left(I_{G2} + \frac{1}{4} m_2 L_2^2 \right) \omega_2^2 + \frac{1}{2} I_{G3} \dot{\theta}_3^2 + \frac{1}{2} m_3 \left[L_2^2 \omega_2^2 + \frac{1}{4} L_3^2 \dot{\theta}_3^2 + L_2 L_3 \omega_2 \dot{\theta}_3 \cos(\theta_2 - \theta_3) \right] + \frac{1}{2}\left(I_{G4} + \frac{1}{4} m_4 L_4^2 \right) \dot{\theta}_4^2 - \frac{1}{2} m_2 g L_2 \sin\theta_2 - m_3 g \left(L_2 \sin\theta_2 + \frac{1}{2} L_3 \theta_3 \right) - \frac{1}{2} m_4 g L_4 \sin\theta_4 \tag{22}$$

Then, differential equations of motion are obtained by using the Lagrange equation for each generalized coordinate and given by,

$$M_2 = \frac{1}{2} m_3 L_2 L_3 \ddot{\theta}_3 \cos(\theta_2 - \theta_3) + \frac{1}{2} m_3 L_2 L_3 \dot{\theta}_3^2 \sin(\theta_2 - \theta_3) + \frac{1}{2} m_2 g L_2 \cos\theta_2 + m_3 g L_2 \cos\theta_2 + L_2 Q_c \sin(\theta_2 - \psi) \tag{23}$$

$$I_{G3} \ddot{\theta}_3 + \frac{1}{4} m_3 L_3^2 \ddot{\theta}_3 - \frac{1}{2} m_3 L_2 L_3 \omega_2^2 \sin(\theta_2 - \theta_3) + \frac{1}{2} m_3 g L_3 \cos\theta_3 = L_3 Q_c \sin(\psi - \theta_3) + \mathrm{R}_B Q_c \sin(\psi - \alpha) \tag{24}$$

$$I_{G4} \ddot{\theta}_4 + \frac{1}{4} m_4 L_4^2 \ddot{\theta}_4 + \frac{1}{2} m_4 g L_4 \cos\theta_4 = L_4 Q_c \sin(\theta_4 - \psi) + \mathrm{R}_J Q_c \sin(\alpha - \psi) \tag{25}$$

where L_i is the length of the i^{th} link and I_{G_i} denotes the inertia moment about the center of mass for each member. M_2 is the required input torque exerted on the crank to maintain its constant angular velocity.

5. Results

Detection of the beginning instant of the contact process is very important for mechanical systems with contact phenomenon. This is for computing the exact initial impact velocity $\dot{\delta}^{(-)}$ and therefore, a variable time step-size algorithm must be utilized. The initial conditions for numerical simulation are based on the results of the kinematic analysis of the four-bar mechanism in which all the joints are assumed to be ideal [31].

The first contact between the journal and the bearing is detected under the following condition:

$$\delta(t_{n-1})\delta(t_n) \le 0 \tag{26}$$

Therefore, the contact may occur between the two discrete times of t_{n-1} and t_n. Since, the continuous contact force model is utilized, this trend continues, regarding the other contact process.

In order to validate the numerical simulation performed in this paper, some results including the follower acceleration, external moment asserting on the crank and the journal center trajectory relative to the bearing center are compared to the numerical results published by Flores et al. [31] (see Fig. 3).

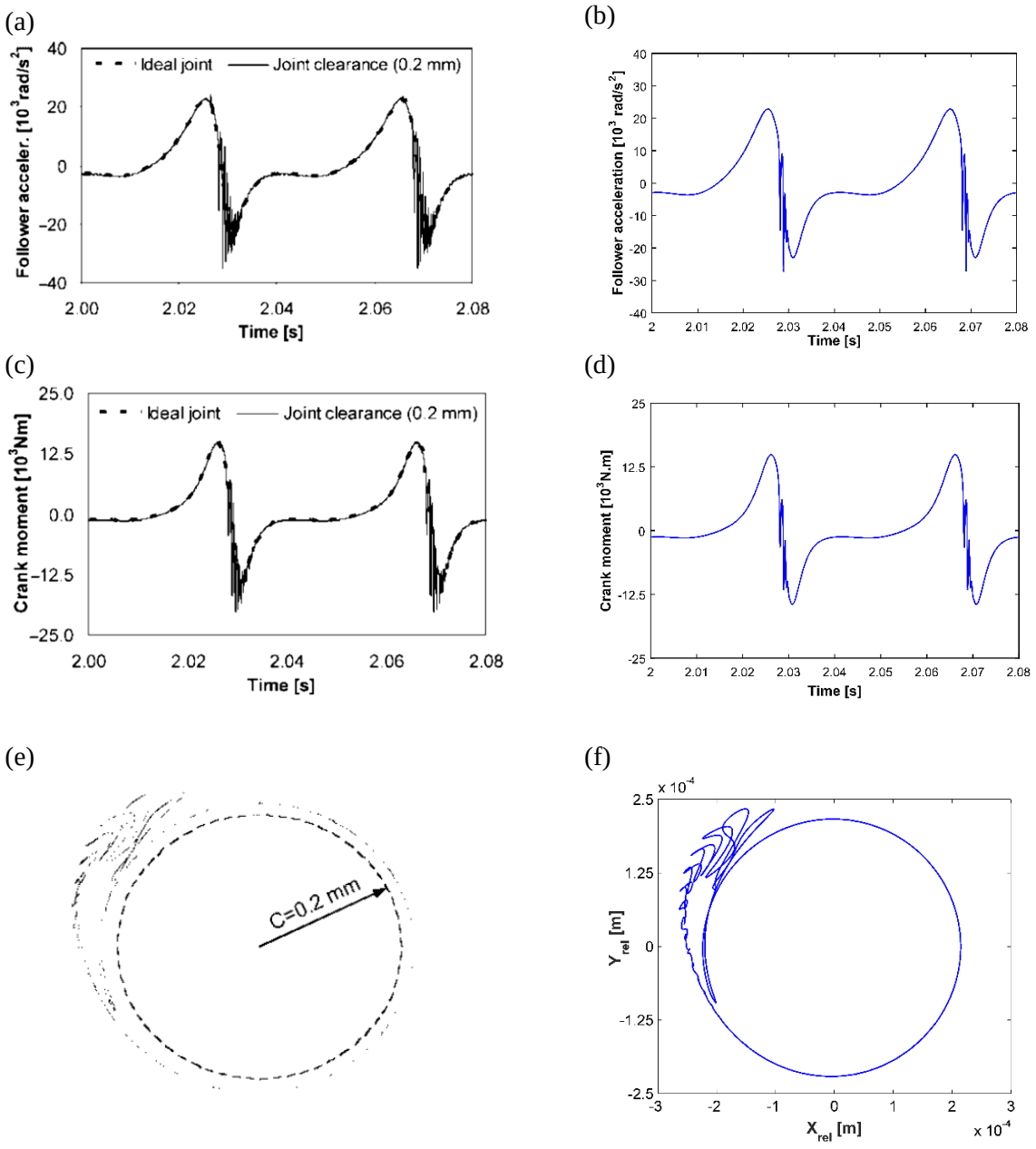

Fig. 3: Numerical results in the present work: (b) follower acceleration, (d) crank moment required to keep the crank angular velocity constant, (f) journal center trajectory relative to bearing center for clearance 0.2mm. (a), (c) and (e) are the corresponding numerical results from Flores [31].

Geometrical and material properties of the linkage required for numerical simulation are listed in Table 1. Erkaya and Uzmay [8] studied the same mechanism with multiple revolute clearance joints.

Table 1: Geometrical and material properties of the mechanism.

Link number	**Mass** (kg)	**Length** (m)	**Inertia moment** (kg·m^2)
1	–	0.8	–
2	0.494	0.25	0.0046
3	1.003	0.75	0.0545
4	0.74	0.45	0.0189

The linkage dynamic behavior for two different crank rotational velocities has been simulated. The clearance size and the friction coefficient between the contact surfaces of the journal and bearing are equal to 0.5 mm and 0.1 mm respectively. The coupler angular acceleration in comparison with the ideal joint and the journal center locus are computed for these two crank angular velocities as shown in Fig. 4. These figures belong to two rotations of the crank. A high peak appears in the rocker acceleration when the impact mode occurs among the joint elements. As the links are rigid, the impact forces are spread through the mechanism and identically appeared as high moment peaks, (Figs. 4a and 4c). When the journal follows the bearing wall and contact loss does not occur, continuous contact mode is governed in the journal-bearing system. Furthermore, this is observed as low amplitude perturbations around the ideal response.

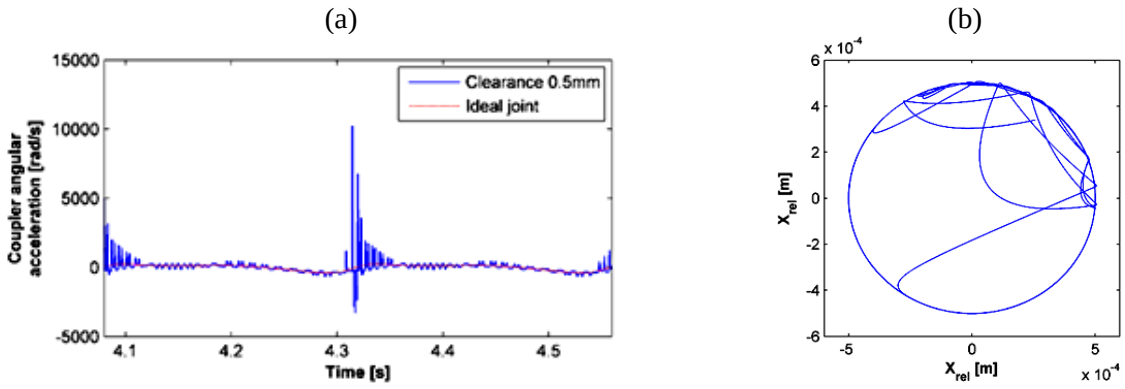

Fig 4: Coupler angular acceleration for: (a) ω=250rpm and (c) ω=3500rpm; Journal center trajectory relative to the bearing center for: (b) ω=250rpm and (d) ω=3500rpm.

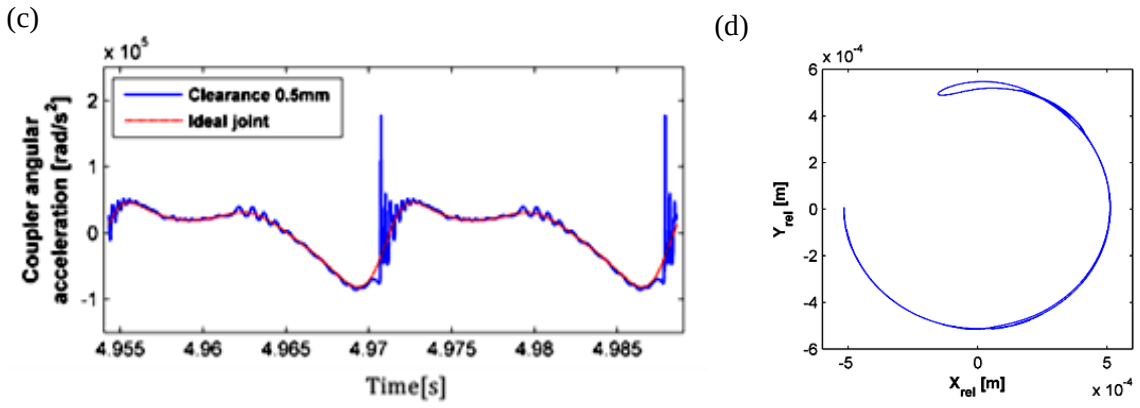

Fig 4: Coupler angular acceleration for: (a) ω=250rpm and (c) ω=3500rpm; Journal center trajectory relative to the bearing center for: (b) ω=250rpm and (d) ω=3500rpm.

At low speed, the high peak points in the coupler acceleration are related to the impact-rebound mode, hence small perturbations around the ideal case refer to the continuous contact mode between the journal and the bearing. When the crank velocity increases, the coupler acceleration amplitude increases and contact loss does not occur since the journal will track the bearing wall forever. It can be seen from Fig. 4d that the journal will not be in contact at some regions of the bearing surface when the mechanism exhibits periodic motion.

In general, impact loads due to joint clearance cause a chaotic behavior in dynamic response of the system. Discrete system behavior is shown in Fig. 5. As illustrated in Figs. 5b and 5c, at low values of the crank speed (250rpm), frequent collisions occur between the joint elements and this leads to chaotic motion. Since the number of points in the Poincaré portraits are infinite, existence of strange attractors or chaos can be deduced in the dynamic response. These figures contain 30000 points. Fractal structure is clearly visible in these figures as the main characteristic of chaotic systems. Fractal means that the geometry has infinite details and self-similar structures at different levels of magnification. A wide output frequency spectrum of the system is another way to detect chaos, while the system input is a harmonic motion with single frequency. In order to represent the system response in the frequency domain, FFT analysis is carried out. For periodic motion, there are differentiable high peaks at the system natural frequency and its harmonics while a wide range of frequencies along with disturbances are visible for chaotic motion. In the case of chaotic motion, frequency response of the system involves disturbances between two consecutive natural frequencies.

Bifurcation diagram, Poincaré portraits and FFT plots are simulated at the speed of 3500 rpm in Fig. 6. The system contains period-one orbit in this clearance size 0.44 mm. In this case, the system response has only one stable fixed point and this will be attracted to the stable limit cycle in continuous phase space when the response reaches it's steady state behavior. For period-one motion, the recognizable peaks in the FFT diagram are just repeated at integer coefficients of the system natural frequency and the plot is smooth in other frequencies (Fig. 6b). The highest peak

is always associated to the natural frequency of the system and its exact value is determined in the figure.

(a)

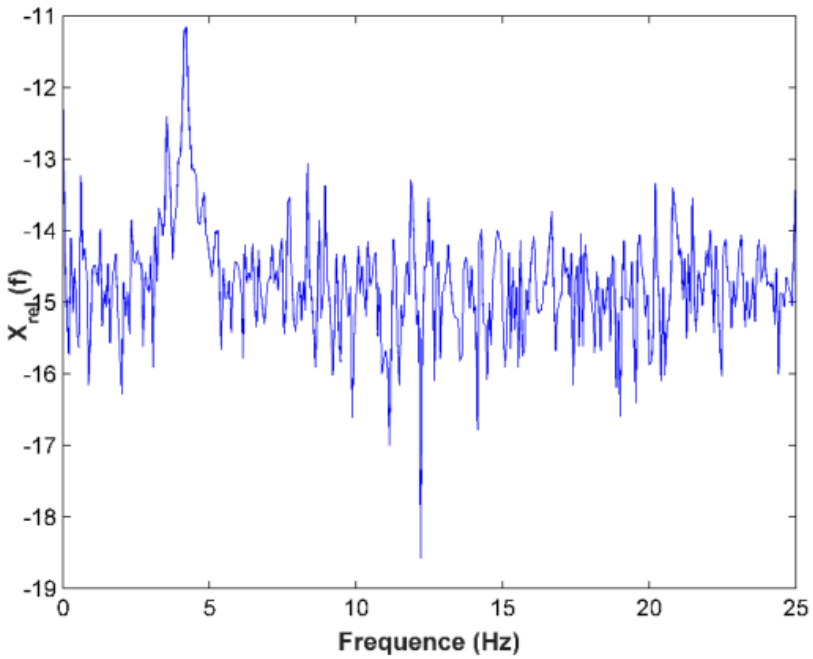

(b)

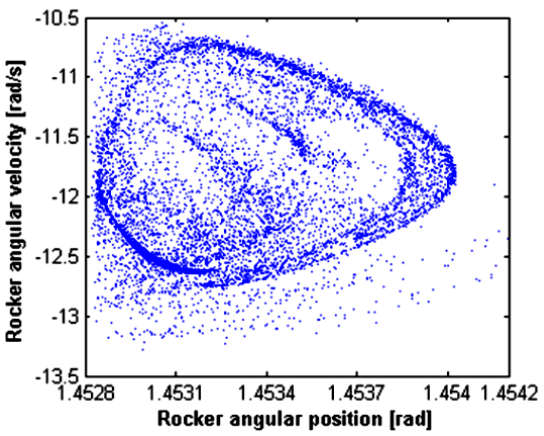

(c)

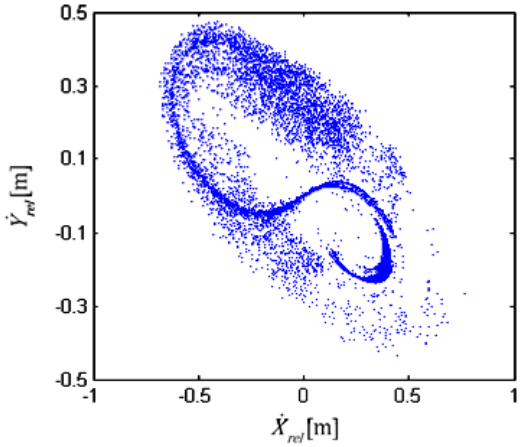

Fig. 5: (a) FFT plot, (b) and (c) Poincaré portraits describing the four-bar linkage behavior for ω=250rpm.

Chaotic and periodic behaviors are also depicted in the continuous phase space in Fig. 7.

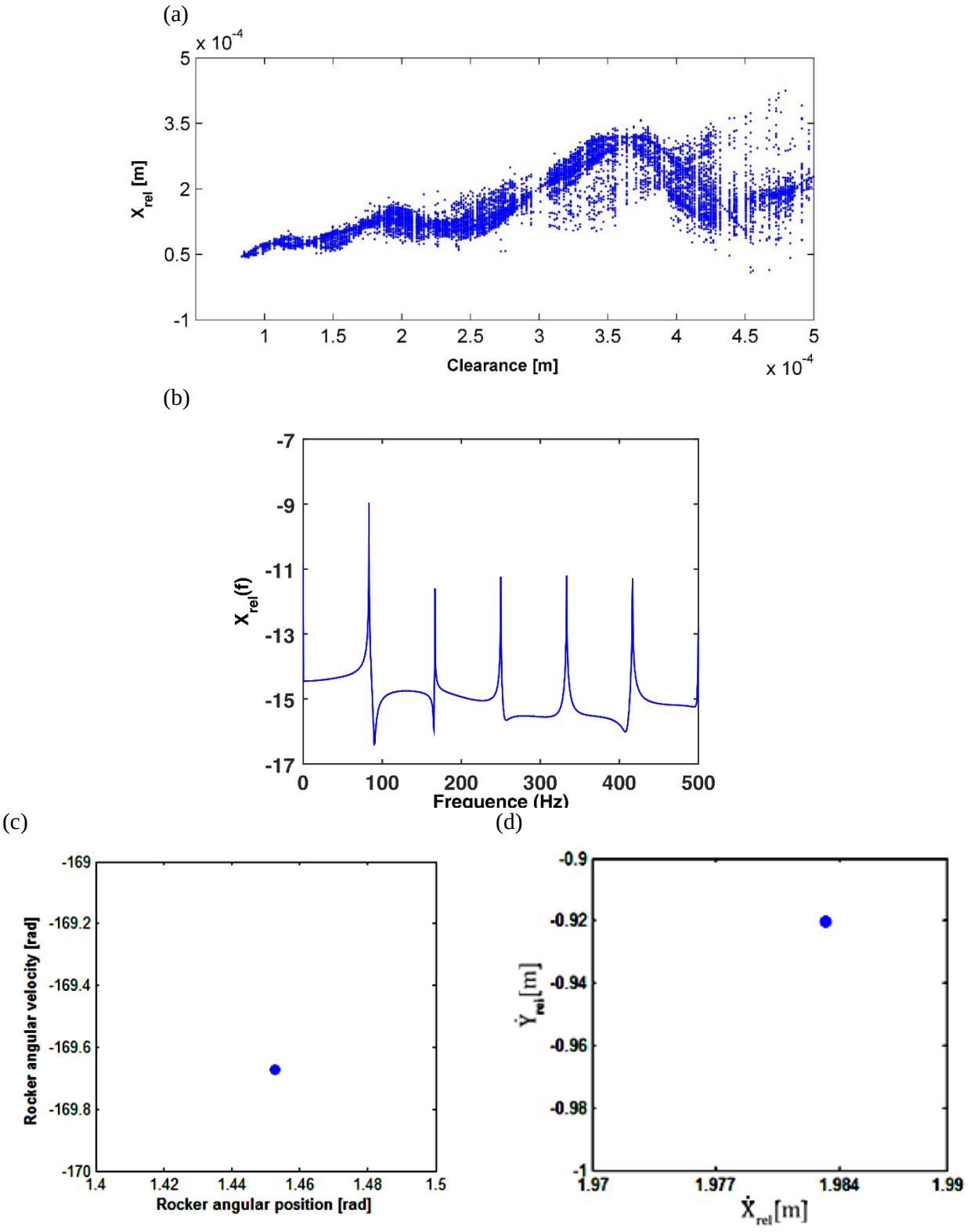

Fig. 6: Bifurcation diagram (a), FFT plot (b) and Poincaré portraits (c-d) describing the four-bar linkage behavior for 3500 rpm

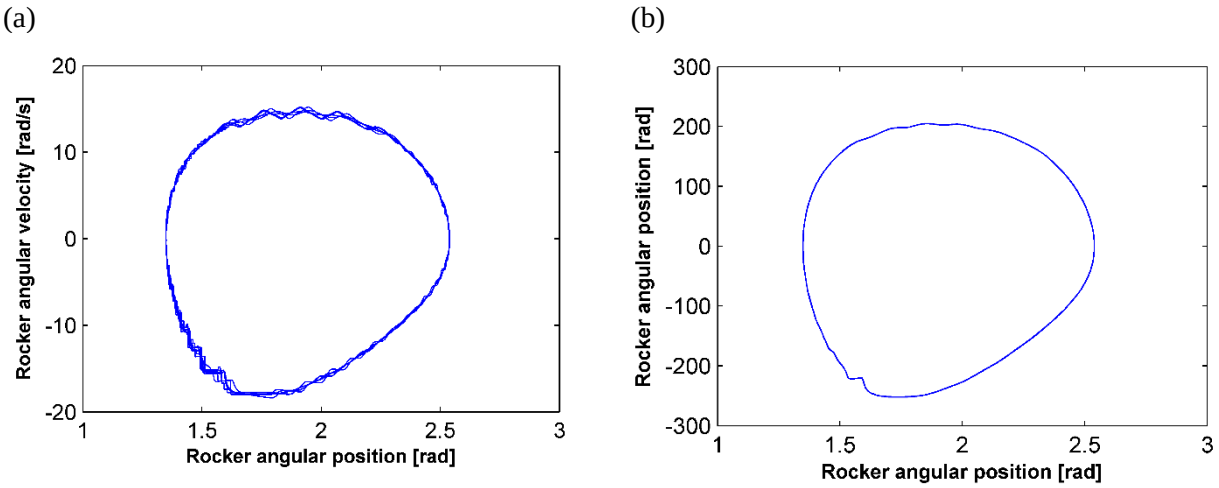

Fig. 7: The continuous state space of system response for: (a) ω=250 rpm, (b) ω=3500 rpm.

6. Conclusion

In this research, nonlinear behavior of a four-bar linkage with clearance is investigated. Differential equations of motion are derived using the Lagrangian approach. Impact and rebound modes between the journal and the bearing lead to high peak points in the coupler acceleration. When the journal follows on the bearing wall, continuous contact mode is occurred and the system response oscillates with slight amplitudes around the ideal case.

Poincaré portrait and FFT analysis are applied to represent the system behavior in the discrete state space and frequency domain respectively. Bifurcation analysis with the change in clearance size is applied for a specific value of the crank angular velocity. Because a four-bar mechanism with clearance is a high-order nonlinear system, more intricate Poincaré mapping figures are expected. Strange attractors or chaos phenomenon can be deduced in the mechanism behavior which are the main characteristics of a chaotic system. As shown, the system response will be attracted to it's period-one orbit embedded in the strange attractors when the crank input velocity increases.

It is observed that the results extracted from FFT analysis and Poincaré phenomena are in precise conformity with those obtained from bifurcation diagrams.

REFERENCES

[1] H.M. Lankarani, P.E. Nikravesh, A contact force model with hysteresis damping for impact analysis of multibody systems, Journal of Mechanical Design, 112 (1990) 369-376.
[2] J.A.C. Ambrósio, Impact of rigid and flexible multibody systems: Deformation description and contact models, Virtual Nonlinear Multibody Systems, 103 (2003) 57-81.
[3] S.M. Varedi, H.M. Daniali, M. Dardel, A. Fathi, Optimal dynamic design of a planar slider-crank mechanism with a joint clearance, Mechanism and Machine Theory, 86 (2015) 191-200.
[4] S. Rahmanian, M.R. Ghazavi, Bifurcation in planar slider–crank mechanism with revolute clearance joint, Mechanism and Machine Theory, 91 (2015) 86-101.

[5] C. Pereira, J. Ambrósio, A. Ramalho, Dynamics of chain drives using a generalized revolute clearance joint formulation, Mechanism and Machine Theory, 92 (2015) 64-85.
[6] S. Erkaya, S. Doğan, Ş. Ulus, Effects of joint clearance on the dynamics of a partly compliant mechanism: Numerical and experimental studies, Mechanism and Machine Theory, 88 (2015) 125-140.
[7] J. Alves, N. Peixinho, M.T. da Silva, P. Flores, H.M. Lankarani, A comparative study of the viscoelastic constitutive models for frictionless contact interfaces in solids, Mechanism and Machine Theory, 85 (2015) 172-188.
[8] S. Erkaya, İ. Uzmay, Modeling and simulation of joint clearance effects on mechanisms having rigid and flexible links, Journal of Mechanical Science and Technology, 28 (2014) 2979-2986.
[9] Y. Tang, Z. Chang, X. Dong, Y. Hu, Z. Yu, Nonlinear dynamics and analysis of a four-bar linkage with clearance, Frontiers of Mechanical Engineering, 8 (2013) 160-168.
[10] G. Chen, H. Wang, Z. Lin, A unified approach to the accuracy analysis of planar parallel manipulators both with input uncertainties and joint clearance, Mechanism and Machine Theory, 64 (2013) 1-17.
[11] A. Azimi Olyaei, M.R. Ghazavi, Stabilizing slider-crank mechanism with clearance joints, Mechanism and Machine Theory, 53 (2012) 17-29.
[12] O. Muvengei, J. Kihiu, B. Ikua, Numerical study of parametric effects on the dynamic response of planar multi-body systems with differently located frictionless revolute clearance joints, Mechanism and Machine Theory, 53 (2012) 30-49.
[13] M. Machado, P. Moreira, P. Flores, H.M. Lankarani, Compliant contact force models in multibody dynamics: Evolution of the Hertz contact theory, Mechanism and Machine Theory, 53 (2012) 99-121.
[14] X. Huang, Y. Zhang, Robust tolerance design for function generation mechanisms with joint clearances, Mechanism and Machine Theory, 45 (2010) 1286-1297.
[15] P. Flores, J. Ambrósio, J.C.P. Claro, H. Lankarani, Spatial revolute joints with clearances for dynamic analysis of multi-body systems, Journal of Multi-body Dynamics, 220 (2006) 257-271.
[16] S. Dubowsky, F. Freudenstein, Dynamic analysis of mechanical systems with clearances—Part 1: Formation of dynamic model, Journal of Engineering for Industry, 93 (1971) 305-309.
[17] S. Dubowsky, T.N. Gardner, Dynamic interactions of link elasticity and clearance connections in planar mechanical systems, Journal of Engineering for Industry, 97 (1975) 652-661.
[18] J. Rhee, A. Akay, Dynamic response of a revolute joint with clearance, Mechanism and Machine Theory, 31 (1996) 121-134.
[19] R.S. Haines, An experimental investigation into the dynamic behaviour of revolute joints with varying degrees of clearance, Mechanism and Machine Theory, 20 (1985) 221-231.
[20] L.D. Seneviratne, S.W.E. Earles, Chaotic behaviour exhibited during contact loss in a clearance joint of a four-bar mechanism, Mechanism and Machine Theory, 27 (1992) 307-321.
[21] A.L. Schwab, J.P. Meijaard, P. Meijers, A comparison of revolute joint clearance models in the dynamic analysis of rigid and elastic mechanical systems, Mechanism and Machine Theory, 37 (2002) 895-913.
[22] P. Flores, J. Ambrósio, J.C.P. Claro, H.M. Lankarani, C.S. Koshy, A study on dynamics of mechanical systems including joints with clearance and lubrication, Mechanism and Machine Theory, 41 (2006) 247-261.

[23] P. Flores, H. Lankarani, J. Ambrósio, C.P. Claro, Modelling lubricated revolute joints in multibody mechanical systems, Journal of Multi-body Dynamics, 218 (2004) 183-190.
[24] P. Flores, H.M. Lankarani, Spatial rigid-multibody systems with lubricated spherical clearance joints: modeling and simulation, Nonlinear Dynamics, 60 (2010) 99-114.
[25] P. Flores, H.M. Lankarani, Dynamic response of multibody systems with multiple clearance joints, Journal of Computational and Nonlinear Dynamics, 7 (2012) 031003.
[26] G.B. Daniel, K.L. Cavalca, Analysis of the dynamics of a slider–crank mechanism with hydrodynamic lubrication in the connecting rod–slider joint clearance, Mechanism and Machine Theory, 46 (2011) 1434-1452.
[27] C.S. Koshy, P. Flores, H.M. Lankarani, Study of the effect of contact force model on the dynamic response of mechanical systems with dry clearance joints: computational and experimental approaches, Nonlinear Dynamics, 73 (2013) 325-338.
[28] Z.F. Bai, Y. Zhao, J. Chen, Dynamics analysis of planar mechanical system considering revolute clearance joint wear, Tribology International, 64 (2013) 85-95.
[29] Q. Tian, Q. Xiao, Y. Sun, H. Hu, H. Liu, P. Flores, Coupling dynamics of a geared multibody system supported by ElastoHydroDynamic lubricated cylindrical joints, Multibody System Dynamics, 33 (2014) 259-284.
[30] E. Askari, P. Flores, D. Dabirrahmani, R. Appleyard, Study of the friction-induced vibration and contact mechanics of artificial hip joints, Tribology International, 70 (2014) 1-10.
[31] P. Flores, J. Ambrósio, J.P. Claro, H.M. Lankarani, Dynamic behaviour of planar rigid multi-body systems including revolute joints with clearance, Proceedings of the Institution of Mechanical Engineers, Part K : Journal of Multi-body Dynamics, 221 (2007) 161-174.